

Effect of transverse beam size on the wakefields and driver beam dynamics in plasma wakefield acceleration schemes

Cite as: AIP Advances 10, 025203 (2020); doi: 10.1063/1.5126210

Submitted: 30 August 2019 • Accepted: 14 January 2020 •

Published Online: 3 February 2020



Ratan Kumar Bera,^{1,a)} Devshree Mandal,¹ Amita Das,² and Sudip Sengupta¹

AFFILIATIONS

¹Institute for Plasma Research, Gandhinagar 382428, Gujarat, India

²Physics Department, Indian Institute of Technology Delhi, Hauz Khas, New Delhi 110016, India

^{a)}Author to whom correspondence should be addressed: rataniitb@gmail.com. Present address: Kevin T. Crofton
Department of Aerospace and Ocean Engineering, Virginia Tech, Blacksburg, VA 24060, USA.

ABSTRACT

In this paper, wakefields driven by a relativistic electron beam in a cold homogeneous plasma are studied using 2D fluid simulation techniques. It has been shown that in the limit when the transverse size of a rigid beam is greater than the longitudinal extension, the wake wave acquires a purely electrostatic form, and the simulation results show a good agreement with the 1D results given by Bera *et al.* [Phys. Plasmas **22**, 073109 (2015)]. In the other limit when the transverse dimensions are equal to or smaller than the longitudinal extension, the wake waves are electromagnetic in nature, and 2D effects play a crucial role. Furthermore, a linear theoretical analysis of 2D wakefields for a rigid bi-parabolic beam has also been carried out and compared with the simulations. It has also been shown that the transformer ratio, which is a key parameter that measures the efficiency in the process of acceleration, becomes higher for a 2D system (i.e., for a beam having a smaller transverse extension compared to the longitudinal length) than the 1D system (i.e., for a beam having a larger transverse extension compared to the longitudinal length). Furthermore, including the self-consistent evolution of the driver beam in the simulation, we have seen that the beam propagating inside the plasma undergoes transverse pinching, which occurs much earlier than the longitudinal modification. Due to the presence of transverse dimensions in the system, the 1D rigidity limit given by Tsiklauri [Phys. Plasmas **25**, 032114 (2018)] gets modified. We have also demonstrated the modified rigidity limit for the driver beam in a 2D beam-plasma system.

© 2020 Author(s). All article content, except where otherwise noted, is licensed under a Creative Commons Attribution (CC BY) license (<http://creativecommons.org/licenses/by/4.0/>). <https://doi.org/10.1063/1.5126210>

I. INTRODUCTION

During the past two decades of research, the plasma wakefield acceleration (PWFA) scheme has unarguably made amazing progress because of its applications, which widely range from medical to industry to high energy physics.^{1–4} The scheme uses extremely large electric fields associated with plasma waves to accelerate charge particles. Typically, these waves, commonly known as a wake wave or wakefield, are created by injecting an ultra-relativistic electron beam inside a plasma. The generation of a strong electric field in a plasma using an ultra-relativistic electron beam stems from the pioneering work by Chen, Dawson, and Huff.⁵ Basically, when an ultra-relativistic electron beam propagates through a plasma, it expels plasma electrons due to space charge force. Ions do not respond

because of their heavy mass. As the beam moves further inside the plasma, these repelled electrons try to come back to their original position. However, due to their inertia, they overshoot, and hence, an oscillation will be established at the back of the beam. As a consequence, a wake wave will be excited at the back of the beam,^{6,7} propagating with a phase velocity equal to the velocity of the beam. These waves, commonly known as wake waves or wakefields, are nothing but the disturbances left behind by the electron beam during propagation inside the plasma. Hence, if a charged particle or beam rides this wave at an appropriate phase, it can be accelerated to high energy using the electric field associated with the wave. As a relativistic electron beam is required even in the first place to excite the wake wave in PWFA, this scheme is not suitable to design a “free-standing” tabletop accelerator. This scheme rather offers a way

to boost the energy of the existing linacs.⁴ Success of this scheme has been demonstrated in a number of experiments^{8–11} by accelerating electrons up to GeV energies. Great progress has also been made in applying the PWFA concept to astrophysical plasmas.^{12–15} Several extensive numerical and analytical works have also been carried out in this area of research. Most of these works have been carried out in 1D where the variations transverse to the beam's directions are ignored.^{16–18} On the other hand, fully 2D nonlinear theoretical works on PWFA have mostly been carried out, ignoring the self-consistent evolution of the driver beam and using special beam profiles.^{19,20} Including the self-consistent evolution of the beam, a detailed characteristic study emphasizing the effect of finite transverse beam size on the wakefield and driver beam dynamics is still largely an unexplored area of research.

In this paper, we report a detailed study of the relativistic electron beam driven wakefield in a cold plasma using 2D fluid simulation techniques. We have performed the simulations over a wide range of beam parameters (i.e., density, velocity, longitudinal length, and transverse length). Here, longitudinal length refers to the length of the beam along the beam direction (longitudinal direction), and transverse length is the length of the beam perpendicular to the beam direction (transverse direction). The simulations have been performed using rigid as well as self-evolving beams. A rigid beam is defined as a beam which can penetrate a long distance inside the plasma without any significant deformation.¹⁷ In this case, the self-consistent evolution of the beam can be ignored. The beam behaves as a rigid piston. For self-evolving beam configuration, the evolution of the beam in the self-consistent fields has been considered. In the simulation, when the transverse dimensions of a rigid bi-Gaussian beam are greater than their longitudinal extension, we have observed that the wake wave excited by the beam acquires a pure electrostatic form. The results obtained from 2D simulation show a good agreement with the 1D results given by Bera *et al.*¹⁷ On the other hand, when the transverse dimensions of a rigid beam are equal to or smaller than their longitudinal extension, the excitations become electromagnetic in nature, and 2D effects play an important part in the dynamics of the beam-plasma system. Furthermore, a linear theoretical analysis of 2D wakefields for a rigid bi-parabolic beam has also been carried out, and the analytical results are compared with the fluid simulations. We have also calculated the transformer ratio, which is a key parameter that measures the efficiency of the acceleration in the simulation. We have observed that the value of the transformer ratio is higher for 2D cases (i.e., for a beam having transverse extension equal to or smaller than its longitudinal length) than 1D systems (i.e., for a beam having transverse extension larger than the longitudinal length). It is to be noted that the transformer ratio for 2D cases is more or less independent of beam density. Including the self-consistent evolution of the driver beam in the simulations [fluid as well as particle-in-cell (PIC)], we have also studied the rigidity of the driver beam. In this paper, PIC simulations are mainly used to support and validate the fluid results. Using both these simulation techniques, it has been shown that the relativistic driver beam propagating through a cold homogeneous plasma undergoes transverse pinching that gives rise to the beam density along the beam direction. We have observed that the transverse pinching attributable to the transverse or focusing fields occurs much earlier than longitudinal modification during the propagation of an ultra-relativistic beam in a plasma. It is also seen that transverse pinching depends

on the beam velocity and occurs later for high beam velocity. Due to pinching in the transverse direction, we have shown that the rigidity limit in terms of beam velocity ($v_b' = 0.9999c$) given by Tsiklauri¹⁸ for 1D cases gets modified. The rigidity limit v_b' is defined as the beam velocity above which the beam can be considered to be rigid for hundreds of plasma periods. We have also shown the modified rigidity limit ($v_b' = 0.999999c$) for a driver beam in a 2D system.

The paper has been organized as follows. In Sec. II, we present the basic equations governing the excitation of a relativistic electron beam driven wakefield in 2D. We have discussed our numerical techniques used for this study in Sec. III. Our numerical observations and the detailed discussion of the obtained results have been covered in Sec. IV. We have summarized our studies in Sec. V.

II. GOVERNING EQUATIONS

The basic equations governing the excitation of a relativistic electron beam driven wakefield in a cold plasma in 2D are the relativistic fluid Maxwell equations. These equations contain continuity and momentum equations for electron beams and plasma electrons. Equations for plasma ions are ignored because of their heavy mass. Maxwell's equations have been used to calculate fields in the system. Therefore, the basic normalized equations for a 2D beam-plasma system can be written as

$$\frac{\partial n}{\partial t} + \vec{\nabla} \cdot (n\vec{v}) = 0, \quad (1)$$

$$\frac{\partial \vec{p}}{\partial t} + (\vec{v} \cdot \vec{\nabla})\vec{p} = -\vec{E} - (\vec{v} \times \vec{B}), \quad (2)$$

$$\frac{\partial n_b}{\partial t} + \vec{\nabla} \cdot (n_b \vec{v}_b) = 0, \quad (3)$$

$$\frac{\partial \vec{p}_b}{\partial t} + (\vec{v}_b \cdot \vec{\nabla})\vec{p}_b = -\vec{E} - (\vec{v}_b \times \vec{B}), \quad (4)$$

$$\frac{\partial \vec{E}}{\partial t} = (n\vec{v} + n_b \vec{v}_b) + (\vec{\nabla} \times \vec{B}), \quad (5)$$

$$\frac{\partial \vec{B}}{\partial t} = -(\vec{\nabla} \times \vec{E}), \quad (6)$$

$$\vec{\nabla} \cdot \vec{E} = (1 - n - n_b), \quad (7)$$

$$\vec{\nabla} \cdot \vec{B} = 0, \quad (8)$$

where $\vec{p} = \gamma\vec{v}$ and $\vec{p}_b = \gamma_b \vec{v}_b$ are the momentum of a plasma electron and a beam electron of velocity \vec{v} and \vec{v}_b , respectively. Here, $\gamma = (1 - v^2)^{-1/2}$ and $\gamma_b = (1 - v_b^2)^{-1/2}$ are the relativistic factors associated with a plasma electron of density n and a beam electron of density n_b , respectively. Other terms \vec{E} and \vec{B} represent the electric and magnetic field, respectively. In the present study, we consider the 2D slab geometry in the (x, z) -plane where the beam is moving along the z -direction. We have used $\vec{\nabla} = \hat{x} \frac{\partial}{\partial x} + \hat{z} \frac{\partial}{\partial z}$, allowing variation in both the longitudinal direction (\hat{z}) and transverse direction (\hat{x}). These equations use the following normalization factors:

$t \rightarrow \omega_{pe} t$, $(x, z) \rightarrow \frac{\omega_{pe}}{c}(x, z)$, $\vec{E} \rightarrow \frac{e\vec{E}}{m_e c \omega_{pe}}$, $\vec{v} \rightarrow \frac{\vec{v}}{c}$, $\vec{v}_b \rightarrow \frac{\vec{v}_b}{c}$, $\vec{p} \rightarrow \frac{\vec{p}}{m_e c}$, $\vec{p}_b \rightarrow \frac{\vec{p}_b}{m_e c}$, $n \rightarrow \frac{n}{n_0}$, $n_i \rightarrow \frac{n_i}{n_0}$, and $n_b \rightarrow \frac{n_b}{n_0}$. Equations (1)–(8) are the main key equations required to examine 2D relativistic electron beam driven wakefield excitation in a cold plasma. The exact analytical solution of these set of equations are formidable. Therefore, we have solved these equations numerically using fluid simulation techniques. For some specific cases, we have also employed fully electromagnetic particle based particle-in-cell (PIC) simulation to compare the results obtained from fluid simulation. In Sec. III, we have discussed both the fluid and PIC simulation techniques used to study the relativistic electron beam driven wakefield in a cold plasma.

III. SIMULATION TECHNIQUES

In this section, we present numerical techniques used to study the relativistic electron beam driven wakefield excitation in a cold plasma. We have used both fluid simulation techniques based on fluid description of the e^- beam–plasma medium and fully kinetic particle based particle-in-cell (PIC) simulation techniques. We have briefly described both the simulation techniques.

A. Fluid simulation of the relativistic electron beam driven wakefield

We have developed a 2D electromagnetic fluid code coupling iteratively a set of subroutines based on the flux-corrected transport (LCPFCT)²¹ scheme, finite-difference time-domain (FDTD) method,²² and successive-over-relaxation (SOR) method.²³ The basic principle of the LCPFCT scheme is based on the generalization of the two-step Lax–Wendroff method.²⁴ The LCPFCT method basically solves generalized continuity type equations. We have used this scheme to solve the continuity and momentum equations, Eqs. (1)–(4), for plasma electrons and electron beams. The FDTD method based on the Yee algorithm has also been implemented to solve Eqs. (5) and (6). The relaxation method has been used to solve Eqs. (7) and (8). In particular, Eqs. (7) and (8) are solved to verify the obtained values of the electric and magnetic field from the simulations. Using this code, we have solved Eqs. (1)–(8) numerically under absorbing boundary conditions in both x - and z -directions for all plasma parameters. The time step (Δt) in the simulations has been chosen using the CFL (Courant–Friedrichs–Lewy) condition²¹ $\Delta t = C_n \Delta S / u_{max}$, where C_n , ΔS , and u_{max} are the Courant number, minimum grid size, and maximum fluid velocity, respectively. In the simulations, we have used $C_n = 0.2$, $\Delta S = \Delta z = \Delta x = 0.05$ as the grid size, where Δz and Δx are the same in both the directions, and $u_{max} = 1$ as the maximum speed is equal to the speed of light. In the simulation, the driver beam is initially kept just inside the plasma with the equilibrium values of plasma profiles at $t = 0$. As time goes, the beam then propagates from one end (left) of the simulation window to its other end (right). As the beam passes the plasma, the wake wave is excited. We note the profile of density and velocity for plasma electrons and beams, and components of the electric field and magnetic field, with time.

B. Particle-in-cell (PIC) simulation of the relativistic electron beam driven wakefield

For some special cases of studies (Subsection IV C), we have used fully kinetic particle based particle-in-cell (PIC) simulation

techniques. We have adopted the fully explicit electromagnetic massively parallel particle based PIC code “OSIRIS 4.0”^{25–27} to study the propagation of electron beams in a plasma. For the same, a 2D slab geometry has been chosen in the $x - z$ plane, where a simulation box of $50 L \times 100 L$ is considered, where $L (=c/\omega_{pe})$ is the skin depth of the plasma. In this box, a bi-Gaussian beam propagating inside a homogeneous plasma along the $+z$ direction with the initial velocity of v_b has been taken. In the simulation, equilibrium plasma density is considered as $n_0 = 10^{21} \text{ cm}^{-3}$. The plasma consists of electrons and ions (immobile) with a very small thermal velocity $v_{th} = 0.000 0442c$. The simulation box has been divided into 5000×2500 cells with 2×2 particles per cell, and the box has absorbing boundary conditions in both directions for particles and fields.

IV. RESULTS AND DISCUSSION

In this section, we present the key results obtained from simulations as well as from analysis. We have mostly used fluid simulation techniques for our study. PIC simulations are used only for studies mentioned in Sec. IV C to emphasize and validate the fluid results for the self-consistent dynamics of the driver beam. The fluid simulations have been performed over a wide range of beam parameters for both the rigid beam and self-evolving beam. In earlier 1D works, it has been shown that the beam can be considered to be rigid if the velocity of the beam $v_b \rightarrow 1$.^{17,18} In this limit, the momentum equation, Eq. (4), for the beam can be ignored, and the dynamics of a rigid beam can be depicted only by Eq. (3) with constant v_b . To implement the rigid beam in the simulation, we have solved Eqs. (1)–(8) except Eq. (4) using $v_b = 0.999 999 99$. We have used rigid beam approximation for the first set of simulations to illustrate the effect of finite transverse beam size on excitation. However, the rigidity of the driver beam is a central question of the plasma wakefield acceleration scheme. For an efficient acceleration process, the driver beam creating the wakefield is required to be rigid for a long distance. But in a real physical system, the driver beam eventually evolves in its self-consistent fields. In the second set of simulations, we have numerically solved the full set of Eqs. (1)–(8) for different beam velocities to study the rigidity limit of the driver beam in 2D. We have presented these simulation results in detail.

A. Effect of transverse beam dimensions on excitation

First, we have studied the effect of the transverse size of the driver beam on the excited wakefield in a cold plasma. We have run fluid simulations using a rigid, bi-Gaussian beam with different values of longitudinal and transverse beam length. The beam velocity (v_b) for all the simulations presented in this subsection (Sec. IV A) is fixed and considered to be 0.999 999 99 (or $\gamma_b = 10 000$). The density profile of the beam has been chosen as

$$n_b = n_{b0} \exp\left(-\frac{(x - \frac{l_x}{2})^2}{2\sigma_x^2}\right) \exp\left(-\frac{z^2}{2\sigma_z^2}\right), \quad (9)$$

where n_{b0} and l_x define the peak density of the beam and the total length of the simulation box along the transverse direction x , respectively. Here, σ_z and σ_x represent the extension or the length of the

beam along the longitudinal and transverse direction, respectively. In Figs. 1 and 2, we show the fluid simulation results obtained for $n_{b0} = 0.1$ at $\omega_{pe}t = 25$. Figure 1 shows the plot of (a) the plasma density profile (n), (b) the longitudinal electric field (E_z), and (c) the transverse magnetic field profile (B_y) for $\sigma_z = 0.5$ and $\sigma_x = \sqrt{15}$. In Fig. 2, we have plotted (a) the plasma density profile (n), (b) the longitudinal electric field (E_z), and (c) the transverse magnetic field profile (B_y) for $\sigma_z = \sqrt{5}$ and $\sigma_x = 0.5$. In subplot (d) of Figs. 1 and 2, we have plotted the profile of the longitudinal electric field (E_z) at the middle of the beam ($x = l_x/2 = 25$) in the transverse direction as a function of z obtained from the fluid simulations along with the 1D analytical results. The 1D results have been obtained from Ref. 16 using the Gaussian beam profile $n_b(z) = n_{b0} \exp(-z^2/(2\sigma_z^2))$. We see that the 2D simulation result shows a good agreement with the 1D results for $\sigma_z = 0.5$ and $\sigma_x = \sqrt{15}$ and deviates for $\sigma_z = \sqrt{5}$ and $\sigma_x = 0.5$. This implies that 1D treatment of the beam-plasma system is valid only for a beam having a long transverse length compared to longitudinal extension. In this case for $\sigma_z/\sigma_x \ll 1$, the nature of the excitations acquires a pure electrostatic form. However, the wakefields become electromagnetic in nature for $\sigma_z/\sigma_x \geq 1$. The 2D effect plays an important role and becomes unavoidable for a beam having a transverse length smaller than its longitudinal extension. Furthermore, for the sake of completeness, an analytical treatment of the 2D linear wakefield has been also carried out. We have discussed the analytical derivation of the linear wakefield for a rigid bi-parabolic beam.

B. Analytical description of 2D wakefields

Here, we present a linear analytical calculation for the electron beam driven wakefield in a cold plasma in 2D. The analytical work has been carried out using a bi-parabolic or an approximated bi-Gaussian beam having a density profile $n_b = n_{b0}(1 - \frac{z^2}{b^2})(1 - \frac{x^2}{a^2})$, where a and b represent the extension of the beam in longitudinal and transverse directions, respectively. Using the frame transformation ($\xi = z - v_b t, x$) and linearizing Eqs. (1)–(6), the evolution of plasma density inside the driver can be written as (see Ref. 28)

$$\partial_\xi^2 n_1(\xi, x) + n_1(\xi, x) = -n_b(\xi, x) = -n_{b0}g(\xi)f(x). \quad (10)$$

The solution of the above equation is

$$n_1 = n_{b0}f(x)G(\xi). \quad (11)$$

Here, $G(\xi) = \int_0^\infty g(\xi') \sin(\xi' - \xi) d\xi'$.

In this frame, the equation for the evolution of longitudinal field is

$$\left(\frac{d^2}{dx^2} - 1\right)(A_{1z} - \phi_1) = -n_1, \quad (12)$$

where ϕ_1 and A_{1z} represent the scalar potential and the z -component of the vector potential, respectively. The solutions of these equations inside the beam can be written as

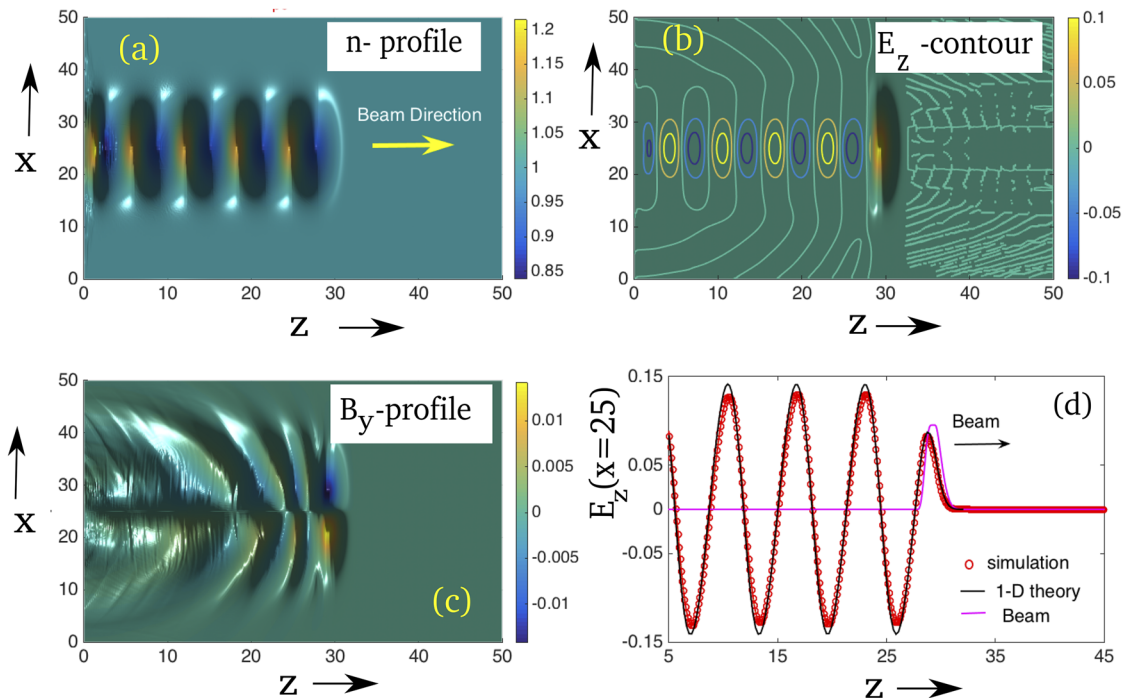


FIG. 1. Plot of (a) normalized plasma electron density (n), (b) longitudinal electric field (E_z), (c) the y -component of the magnetic field (B_y), and (d) the profile of E_z at $x = l_x/2$ as a function of z from simulation (red circle) and 1D theory (black solid line) at $\omega_{pe}t = 25$ for the normalized peak beam density (n_b) = 0.1, $\sigma_z = 0.5$, $\sigma_x = \sqrt{15}$, and beam velocity (v_b) = 0.999 999 99.

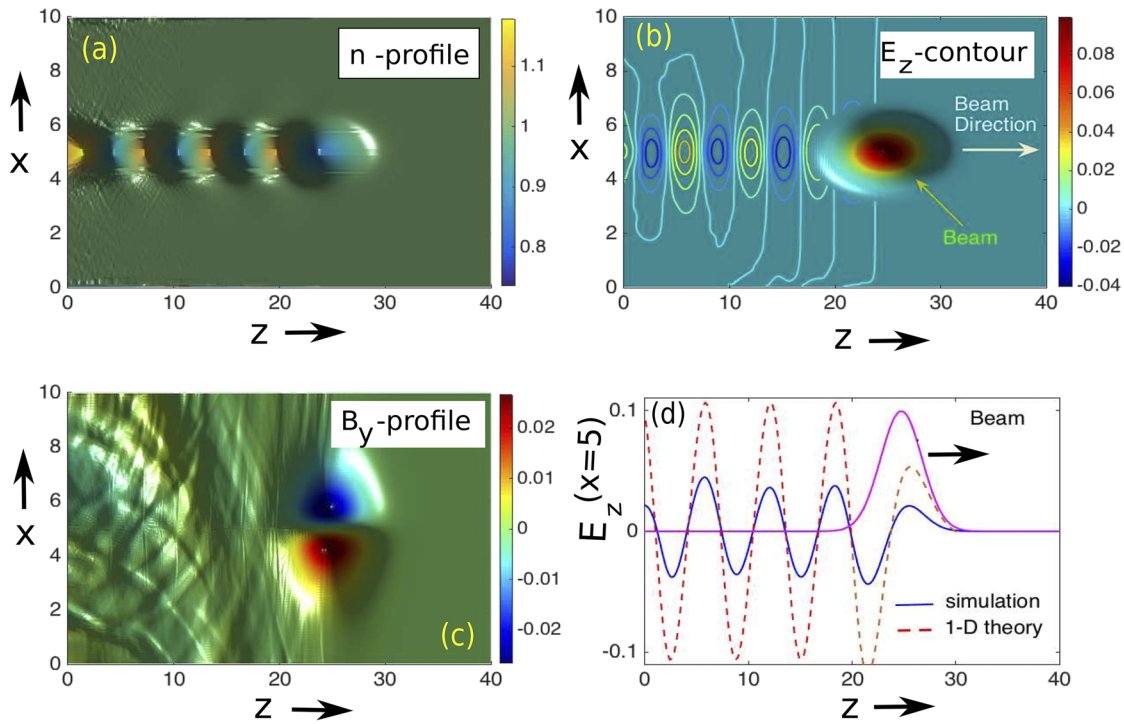


FIG. 2. Plot of (a) normalized plasma electron density (n), (b) longitudinal electric field (E_z), (c) the y -component of the magnetic field (B_y), and (d) the profile of E_z at $x = l_x/2$ as a function of z from simulation (blue solid line) and 1D theory (red dotted line) at $\omega_{pe}t = 25$ for the normalized peak beam density ($n_b = 0.1$), $\sigma_z = \sqrt{5}$, $\sigma_x = 0.5$, and beam velocity ($v_b = 0.999\,999\,99$).

$$(A_{1z} - \phi_1) = -n_{b0}G(\xi)F(x). \quad (13)$$

For the bi-parabolic beam profile, it is quite straightforward to find the value of $F(x)$ and $G(\xi)$. Therefore, the solutions of these equations can be written as

$$(A_{1z} - \phi_1) = -2n_{b0} \left[\frac{2}{a^2} + \frac{x^2}{a^2} - 1 \right] \left[\left(1 - \frac{(\xi + b)^2}{b^2} \right) + \frac{2}{b} \sin(\xi) + \frac{2}{b^2} (1 - \cos(\xi)) \right]. \quad (14)$$

The expression of the longitudinal electric field inside the beam is

$$E_z = \frac{\partial}{\partial \xi} (A_{1z} - \phi_1) = -2n_{b0} \left[\frac{2}{a^2} + \frac{x^2}{a^2} - 1 \right] \left[\left(-\frac{2(\xi + b)}{b^2} \right) + \frac{2}{b} \cos(\xi) + \frac{2}{b^2} \sin(\xi) \right]. \quad (15)$$

At the wake of the beam ($n_b = 0$), the solution of Eq. (10) can be written as

$$n_1 = A(x) \sin(\xi) + B(x) \cos(\xi). \quad (16)$$

Here, $A(x) = n_{b0}F(x) (G(\xi_f)\sin(\xi_f) + G'(\xi_f)\cos(\xi_f))$ and $B(x) = n_{b0}F(x)G'(\xi_f) - \frac{A(y)}{F(x)\tan(\xi_f)}$, where ξ_f represents the value of ξ at the end of the beam. Thus, the longitudinal electric field at the wake of the beam can be derived as

$$E_z(\xi, x) = -2A(x) \cos(\xi) - 2B(x) \sin(\xi). \quad (17)$$

Using the bi-parabolic beam with peak beam density $n_{b0} = 0.1$ and velocity $v_b = 0.999\,999\,99$, we have also performed fluid simulation for different values of longitudinal and transverse beam length. The simulation results are shown in Figs. 3 and 4. Figure 3 shows the profile of (a) plasma density (n), (b) longitudinal electric field (E_z), and (c) beam density (n_b) for $b = 0.5$ and $a = \sqrt{15}$ at $\omega_{pe}t = 25$. Figure 4 shows the profile of (a) plasma density (n), (b) longitudinal electric field (E_z), and (c) transverse magnetic field profile (B_y) for $b = \sqrt{5}$ and $a = 0.5$ at $\omega_{pe}t = 18$. For these two cases, the ratio between longitudinal length to transverse length is $b/a = 0.129 < 1$ and $l_s = b/a = 4.4 > 1$, respectively. In the last subplots of Figs. 3(d) and 4(d), we have plotted the profile of the longitudinal electric field at $x = l_x/2$ as a function of z obtained from our simulation along with the profiles obtained from 2D linear analytical results obtained by solving Eq. (17) and the corresponding 1D theoretical profile obtained from Ref. 16. We have observed that our simulation result matches with the 2D theoretical results for all ratios of b/a . The profile of longitudinal electric field obtained from both 2D simulation and 2D theory deviates from 1D theory results for $b/a = 4.4 > 1$. This implies that the extension of the beam decides the dimension of analysis for the beam-plasma system. Earlier 1D analysis of the beam-plasma system^{5,17,18} is only valid for a long transverse beam compared to its longitudinal extension.

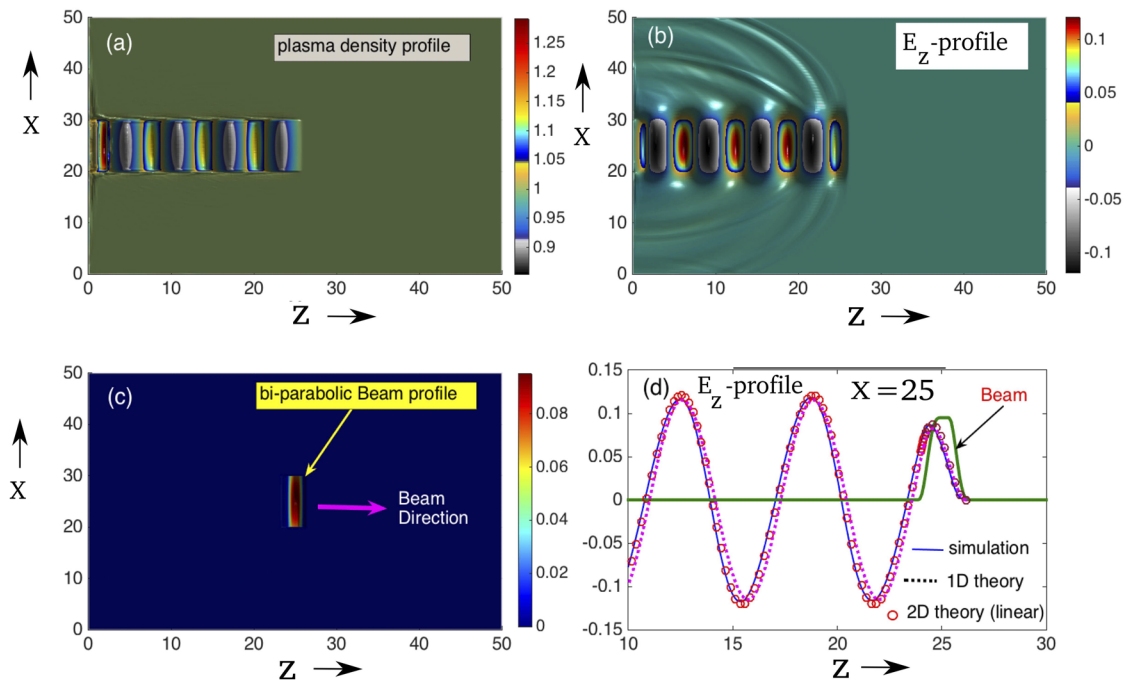


FIG. 3. Plot of (a) normalized plasma electron density (n), (b) longitudinal electric field (E_z), (c) the beam (n_b), and (d) the profile of E_z at $x = l_x/2$ as a function of z from simulation (blue solid line), 2D theory (red circle), and 1D theory (magenta dotted line) at $\omega_{pe}t = 25$ for the normalized peak beam density (n_b) = 0.1, $b = 0.5$, $a = \sqrt{15}$, and beam velocity (v_b) = 0.999 999 99.

Furthermore, we have also calculated the transformer ratio using a bi-parabolic beam for both 1D (beam having $\sigma_z/\sigma_x \ll 1$) and 2D ($\sigma_z/\sigma_x \geq 1$) systems. In general, the transformer ratio (R) is defined as $R = E_z^-/E_z^+$, where E_z^- and E_z^+ are the maximum accelerating longitudinal electric field outside the beam and maximum decelerating longitudinal electric field inside the beam, respectively. We have calculated the values of R from the simulation using a bi-parabolic beam of different length ratios (σ_z/σ_x). In Fig. 5, we have plotted the transformer ratio as a function of different beam densities (n_b) both for $\sigma_z/\sigma_x = 0.5/3.87 \ll 1$ and $\sigma_z/\sigma_x = 0.5/0.5 = 1$. Clearly, the excitation for $\sigma_z/\sigma_x \ll 1$ will be purely electrostatic or 1D, and the excitations will be electromagnetic in nature for $\sigma_z/\sigma_x = 1$. We see that the transformer ratio obtained for 2D cases is higher than that obtained in 1D cases. It is also observed that the transformer ratio is nearly independent of the beam density for 2D cases, whereas the transformer ratio in 1D cases monotonically decreases after a certain density (see also Ref. 17).

C. Self-consistent evolution of the driver beam

The results presented so far have been obtained using a rigid beam. This implies the charge density and energy of the beam remain constant throughout the propagation. However, in a realistic situation, the beam propagating inside the plasma must lose its energy and must be evolved in its self-consistent fields. To avoid beam deformation or self-consistent evolution of the beam inside the plasma, most of the analysis of PWFA uses a beam velocity equal

or very close to the speed of light. Including the self-consistent evolution of the beam, several authors also have extensively studied the beam dynamics in a plasma in 1D and reported a critical beam velocity v_b^* above which the beam can be considered to be rigid.^{17,18} Recently, using 1D PIC simulation, Tsiklauri¹⁸ established that the driver beam would behave rigid when the velocity of the beam $v_b \geq 0.9999$ or $\gamma_b \geq 70.7$.

In this subsection, we present a detailed investigation on the rigidity of the driver beam including the self-consistent evolution in 2D. We have performed both fluid and PIC simulations to study the driver beam dynamics in a plasma. In the fluid simulation, we have solved the full set of Eqs. (1)–(8) using a bi-Gaussian beam profile defined by Eq. (9) for different beam velocities. In the PIC simulations, we have also used the same beam and plasma profiles and parameters. The details of the PIC simulation techniques used here are described in Sec. III. PIC simulations are mainly used to verify the fluid results as analytical solution of the full set of Eqs. (1)–(8) is difficult. The simulation results are presented in Figs. 6 and 7 for a bi-Gaussian beam having $n_{b0} = 0.3$, $\sigma_z = 0.5$, and $\sigma_x = \sqrt{15}$. Therefore, we have performed simulations for 1D cases as $\sigma_z/\sigma_x \ll 1$. In Fig. 6(a), we have plotted the driver beam density profile at different times obtained from fluid simulation for beam velocities $v_b = 0.9999$ or $\gamma_b = 70.7$ (top) and $v_b = 0.999999$ or $\gamma_b = 707.1$ (bottom). In Fig. 6(b) we have shown the driver beam density profile at different times obtained from PIC simulation for beam velocities $v_b = 0.9999$ or $\gamma_b = 70.7$ (top) and $v_b = 0.999999$ or $\gamma_b = 707.1$ (bottom). It is evident from both these simulations that the beam profile

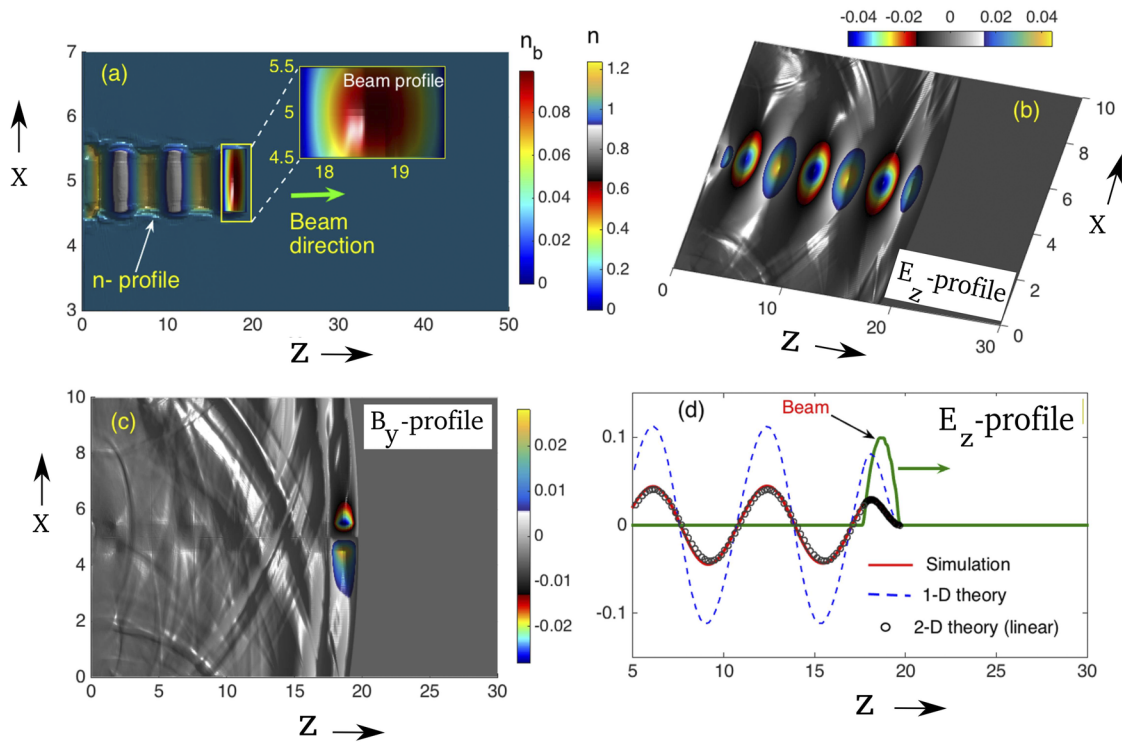


FIG. 4. Plot of (a) normalized plasma electron density (n), (b) longitudinal electric field (E_z), (c) the y -component of the magnetic field (B_y), and (d) the profile of E_z at $x = l_x/2$ as a function of z from simulation (red solid line), 2D theory (black circle), and 1D theory (blue dotted line) at $\omega_{pe}t = 17$ for the normalized peak beam density (n_b) = 0.1, $b = \sqrt{5}$, $a = 0.5$, and beam velocity (v_b) = 0.999 999 99.

gets modified for $v_b = 0.9999$ within 100 plasma periods even for a long transverse beam, whereas it can be considered to be rigid for $v_b = 0.999\,999$ or $v_b = 707.1$. We note that the results presented here are in contrast with the results given by Tsiklauri.¹⁸ This is due to

the presence of transverse dimension in the simulations. Tsiklauri, using 1D PIC simulation, showed that the beam having velocity $v_b = 0.9999$ must be rigid for hundreds of plasma periods inside a plasma. They have deliberately restricted the dynamics of the beam

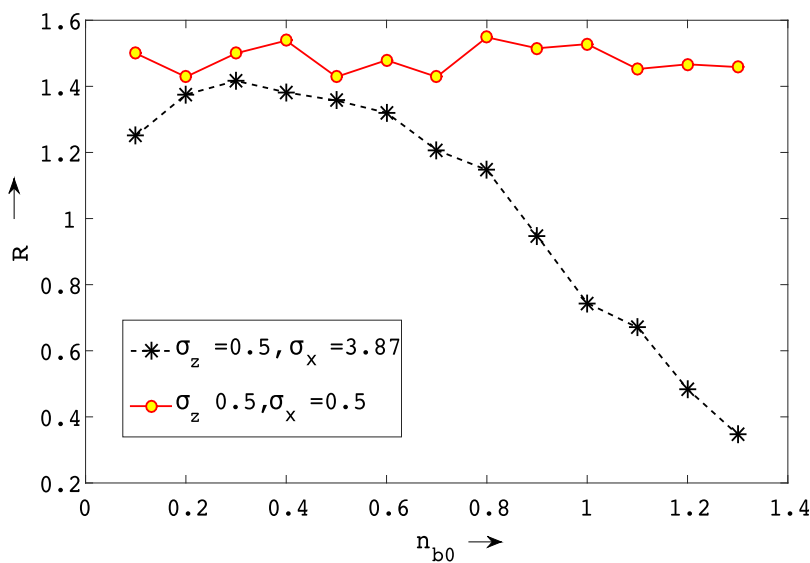


FIG. 5. Plot of the transformer ratio (R) as a function of peak beam density (n_{b0}) for the 1D case ($\sigma_z = 0.5$, $\sigma_x = \sqrt{15}$) and 2D case ($\sigma_z = 0.5$, $\sigma_x = 0.5$).

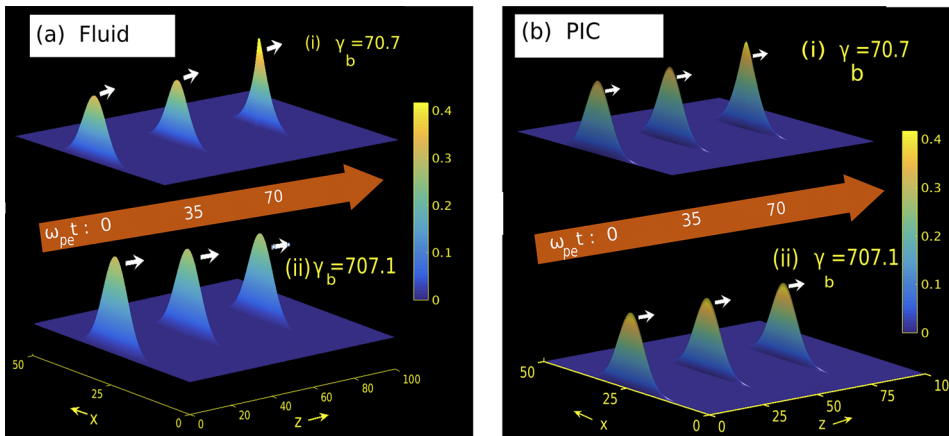


FIG. 6. Plot of the beam density profile (n_b) having $n_{b0} = 0.3$, $\sigma_z = 0.5$, and $\sigma_x = \sqrt{15}$ at different times for $\gamma_b = 70.7$ and $\gamma_b = 707.1$ using (a) fluid simulation and (b) PIC simulation. Subplots (a-i) and (b-i) represent the beam evolution for $\gamma_b = 70.7$ in fluid and PIC simulation, respectively. Subplots (a-ii) and (b-ii) represent the beam evolution for $\gamma_b = 707.1$ in fluid and PIC simulation, respectively.

only to one dimension, ignoring the variation in the transverse direction. Although the effective dimension of the problem is still 1D (as $\sigma_z/\sigma_x \ll 1$), due to the presence of transverse variation in the simulation, the beam having finite transverse extension gets modified. In a real physical system, we always have a beam of finite extensions. Due to the finite transverse extension which can be much larger than longitudinal length, the evolution of the beam acquires an additional modification by the transverse dynamics.

To understand the beam evolution in detail, we have also plotted the beam profiles in Fig. 7 in both longitudinal and transverse directions from both the fluid and PIC simulation. In Fig. 7, we have plotted the beam profiles at different times for $\gamma_b = 70.7$ and $\gamma_b = 707.1$. In Fig. 7(a), we show the beam density profile (n_b) at $x = l_x/2 = 25$ as a function of z obtained from both fluid and PIC simulation at different times for $\gamma_b = 70.7$. Figure 7(b) plots the beam density profile (n_b) at $z = z_t$ as a function of x obtained from both fluid and PIC simulation at different times for $\gamma_b = 70.7$. Here, z_t

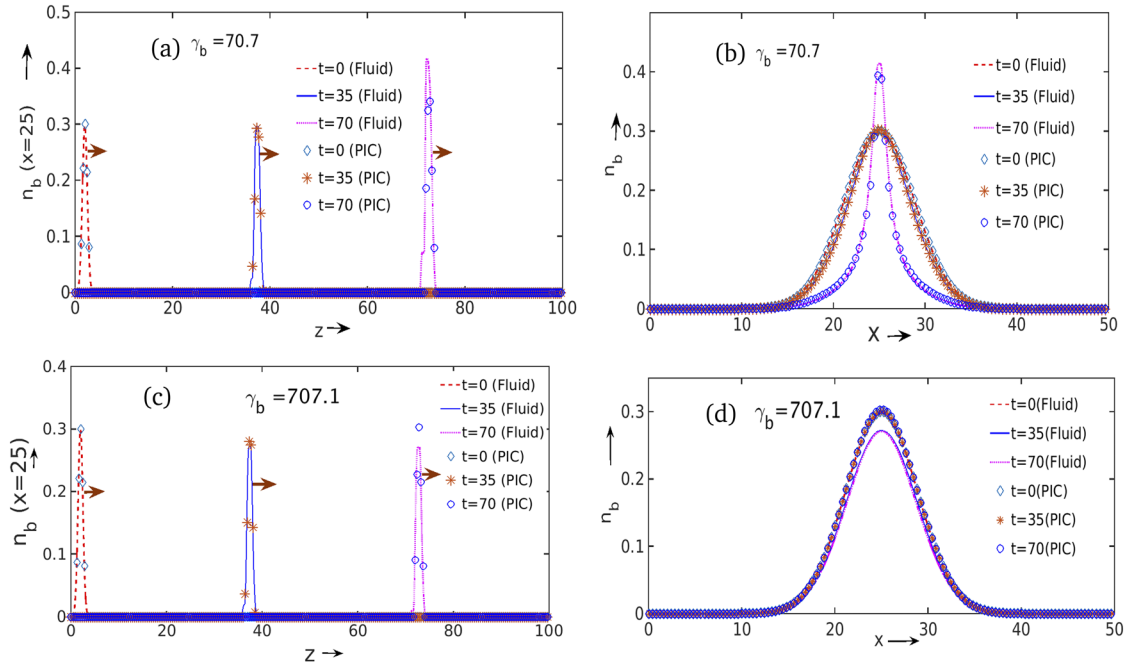


FIG. 7. Plot of (a) the beam density profile (n_b) at $x = l_x/2 = 25$ as a function of z obtained from both fluid and PIC simulation at different times for $\gamma_b = 70.7$, (b) the beam density profile (n_b) at z_t (value of z at the peak of the beam) as a function of x obtained from both fluid and PIC simulation at different times for $\gamma_b = 70.7$, (c) the beam density profile (n_b) obtained from both fluid and PIC simulation as a function of z at different times for $\gamma_b = 707.1$, and (d) the beam density profile (n_b) at z_t (value of z at the peak of the beam) as a function of x obtained from both fluid and PIC simulation at different times for $\gamma_b = 707.1$.

defines the value of z where the peak of the beam lies at different times. In Fig. 7(c), we have plotted the beam density profile (n_b) at $x = l_x/2 = 25$ as a function of z obtained from both fluid and PIC simulation at different times for $\gamma_b = 707.1$. Figure 7 shows the beam density profile (n_b) at $z = z_t$ as a function of x obtained from both fluid and PIC simulation at different times for $\gamma_b = 707.1$. We see that the beam undergoes transverse pinching during propagation inside a plasma. Transverse pinching is a well known phenomenon in a relativistic beam-plasma system.²⁹ Transverse pinching occurs due to the finite size in the transverse direction. Because of finiteness, the system possesses a radial wakefield or focusing fields that gradually pinch the beam. As a consequence, the density of the beam increases along the longitudinal direction. It is seen that the longitudinal length of the beam remains unchanged for both $v_b = 0.9999$ and $v_b = 0.999999$. We also note that transverse pinching modifying the beam profile depends on the beam velocity. For high beam velocity, a significant pinching occurs at later times. We see that the effect of transverse pinching is negligibly small for hundreds of plasma periods for $v_b = 0.999999$ and the beam is rigid. The results presented in Subsection IV A using the rigid beam are consistent with these studies as they are obtained for $v_b = 0.99999999$ or $\gamma_b = 10\,000$.

V. CONCLUSION

This paper reports a detailed study of electron beam driven wakefields in a cold plasma in 2D using fluid as well as particle-in-cell (PIC) simulation techniques. It has been shown that in the limit when the transverse dimensions of a rigid bi-Gaussian beam are greater than their longitudinal extension, the wake wave excited by the beam acquires a pure electrostatic form, and the simulation results show a good agreement with the 1D results given by Bera *et al.*¹⁷ In the other limit, when the transverse dimensions of a rigid beam are equal to or smaller than their longitudinal extension, the wakefields become electromagnetic in nature. Furthermore, a linear theoretical analysis of 2D wakefields has been carried out for a rigid bi-parabolic beam, and the results have been verified with the simulations. The transformer ratio, which is a key parameter for measuring the efficiency of the acceleration in PWFA, is found to be larger for 2D cases than that obtained from 1D systems. Including the self-consistent beam evolution in the simulation, we have studied the driver beam dynamics in a 2D system. It has been shown that the rigidity limit of the driver beam obtained from purely 1D simulation systems gets modified due to the presence of transverse dimension. The relativistic beam propagating inside the plasma gets pinched in the transverse dimension. We have also obtained and demonstrated the modified rigidity limit for the driver beam in the PWFA concept.

ACKNOWLEDGMENTS

The authors are grateful to the IPR computer center where the simulation studies presented in this paper were carried out. A.D. and D.M. would like to acknowledge the OSIRIS Consortium, consisting of UCLA and IST (Lisbon, Portugal), for providing access to the OSIRIS 4.0 framework.^{26,27}

REFERENCES

- E. Gschwendtner and P. Muggli, "Plasma wakefield accelerators," *Nat. Rev. Phys.* **1**, 246–248 (2019).
- C. Jing, "Dielectric wakefield accelerators," *Rev. Accel. Sci. Technol.* **09**, 127 (2016).
- E. Esarey, C. B. Schroeder, and W. P. Leemans, "Physics of laser-driven plasma-based electron accelerators," *Rev. Mod. Phys.* **81**, 1229 (2009).
- J. L. Miller, "Plasma wakefield acceleration shows promise," *Phys. Today* **68**(1), 11 (2015).
- P. Chen, J. M. Dawson, W. R. Huff, and T. Katsouleas, "Acceleration of electrons by the interaction of a bunched electron beam with a plasma," *Phys. Rev. Lett.* **54**, 693 (1985).
- C. Joshi and V. Malka, "Focus on laser- and beam-driven plasma accelerators," *New J. Phys.* **12**, 045003 (2010).
- T. Katsouleas, "Physical mechanisms in the plasma wake-field accelerator," *Phys. Rev. A* **33**, 2056 (1986).
- M. J. Hogan, C. D. Barnes, C. E. Clayton, F. J. Decker, S. Deng, P. Emma, C. Huang, R. H. Iverson, D. K. Johnson, C. Joshi, T. Katsouleas, P. Krejcik, W. Lu, K. A. Marsh, W. B. Mori, P. Muggli, C. L. O'Connell, E. Oz, R. H. Siemann, and D. Walz, "Multi-GeV energy gain in a plasma-wakefield accelerator," *Phys. Rev. Lett.* **95**, 054802 (2005).
- G. Xia, D. Angal-Kalinin, J. Clarke, J. Smith, E. Cormier-Michel, J. Jones, P. H. Williams, J. W. McKenzie, B. L. Militsyn, K. Hanahoe, O. Mete, A. Aimidula, and C. P. Welsch, "A plasma wakefield acceleration experiment using CLARA beam," *Nucl. Instrum. Methods Phys. Res., Sect. A* **775**, 168 (2015).
- I. Blumenfeld, C. E. Clayton, F.-J. Decker, M. J. Hogan, C. Huang, R. Ischebeck, R. Iverson, C. Joshi, T. Katsouleas, N. Kirby, W. Lu, K. A. Marsh, W. B. Mori, P. Muggli, E. Oz, R. H. Siemann, D. Walz, and M. Zhou, "Energy doubling of 42 GeV electrons in a metre-scale plasma wakefield accelerator," *Nature* **445**, 741 (2007).
- M. Litos, E. Adli, W. An, C. I. Clarke, C. E. Clayton, S. Corde, J. P. Delahaye, R. J. England, A. S. Fisher, J. Frederico, S. Gessner, S. Z. Green, M. J. Hogan, C. Joshi, W. Lu, K. A. Marsh, W. B. Mori, P. Muggli, N. Vafaei-Najafabadi, D. Walz, G. White, Z. Wu, V. Yakimenko, and G. Yocky, "High-efficiency acceleration of an electron beam in a plasma wakefield accelerator," *Nature* **515**, 92 (2014).
- D. Tsiklauri, "Electron plasma wake field acceleration in solar coronal and chromospheric plasmas," *Phys. Plasmas* **24**, 072902 (2017).
- D. Tsiklauri, "Collisionless, phase-mixed, dispersive, Gaussian Alfvén pulse in transversely inhomogeneous plasma," *Phys. Plasmas* **23**, 122906 (2016).
- T. Ebisuzaki and T. Tajima, "Astrophysical ZeV acceleration in the relativistic jet from an accreting supermassive blackhole," *Astropart. Phys.* **56**, 9–15 (2014).
- P. Chen, T. Tajima, and Y. Takahashi, "Plasma wakefield acceleration for ultrahigh-energy cosmic rays," *Phys. Rev. Lett.* **89**, 161101 (2002).
- J. B. Rosenzweig, "Nonlinear plasma dynamics in the plasma wake-field accelerator," *Phys. Rev. Lett.* **58**, 555 (1987).
- R. K. Bera, S. Sengupta, and A. Das, "Fluid simulation of relativistic electron beam driven wakefield in a cold plasma," *Phys. Plasmas* **22**, 073109 (2015).
- D. Tsiklauri, "Differences in 1D electron plasma wake field acceleration in MeV versus GeV and linear versus blowout regimes," *Phys. Plasmas* **25**, 032114 (2018).
- W. Lu, C. Huang, M. Zhou, M. Tzoufras, F. S. Tsung, W. B. Mori, and T. Katsouleas, "A nonlinear theory for multidimensional relativistic plasma wave wakefields," *Phys. Plasmas* **13**, 056709 (2006).
- S. S. Baturin, G. Andonian, and J. B. Rosenzweig, "Analytical treatment of the wakefields driven by transversely shaped beams in a planar slow-wave structure," *Phys. Rev. Accel. Beams* **21**, 121302 (2018).
- J. P. Boris, A. M. Landsberg, E. S. Oran, and J. H. Gardner, "LCPFCT—Flux-corrected transport algorithm for solving generalized continuity equations," Report No. NRL/MR/6410-93-7192, Naval Research Laboratory, Washington, 1993.
- U. S. Inan and R. A. Marshall, *Numerical Electromagnetics: The FDTD Method* (Cambridge University Press, 2011).

- ²³A. Hadjidimos, "Successive overrelaxation (SOR) and related methods," *J. Comput. Appl. Math.* **123**, 177–199 (2000).
- ²⁴W. Press, R. Assmann, A. Teukolsky, W. Vetterling, and B. P. Flannery, *Numerical Recipes: The Art of Scientific Computing* (Cambridge University Press, 1992).
- ²⁵R. G. Hemker, "Particle-in-cell modeling of plasma-based accelerators in two and three dimensions," Ph.D. thesis, University of California, Los Angeles, 2000 (Physics—Computational Physics, Physics—Plasma Physics).
- ²⁶R. A. Fonseca, L. O. Silva, F. S. Tsung, V. K. Decyk, W. Lu, C. Ren, W. B. Mori, S. Deng, S. Lee, T. Katsouleas, and J. C. Adam, "Osiris: A three-dimensional, fully relativistic particle in cell code for modeling plasma based accelerators," in *Computational Science — ICCS 2002*, International Conference, Amsterdam, The Netherlands, April 21–24, 2002 Proceedings, Part III.
- ²⁷R. A. Fonseca, S. F. Martins, L. O. Silva, J. W. Tonge, F. S. Tsung, and W. B. Mori, "One-to-one direct modeling of experiments and astrophysical scenarios: Pushing the envelope on kinetic plasma simulations," *Plasma Phys. Controlled Fusion* **50**(12), 124034 (2008).
- ²⁸P. Chen, "A possible final focusing mechanism for linear colliders," SLAC-PUB-3823 (Rev.), SLAC/AP-46 (A/AP), November 1985.
- ²⁹R. Keinigs and M. E. Jones, "Two-dimensional dynamics of the plasma wakefield accelerator," *Phys. Fluids* **30**, 252 (1987).